J3.5

COUPLING LAGRANGIAN SURFACE LAYER AND CONVECTIVE BOUNDARY LAYER MODELS TO DESCRIBE AERIAL DISPERSAL OF PARTICLES RELEASED NEAR THE GROUND

Matthew T. Boehm* and Donald E. Aylor
The Connecticut Agricultural Experiment Station, New Haven, Connecticut

1. INTRODUCTION

The inadvertent introduction of exotic pathogens (such as the soybean rust pathogen) and the seasonal reintroduction to northern latitudes of diseases (such as tobacco blue mold) reinforce the need for better spore dispersal models because of the potential economic impact of local and inter-regional spread of plant diseases. Likewise, the extensive adoption of genetically modified crops has led to a need to better understand the dispersal of pollen in the atmosphere because of the potential for unwanted movement of genetic traits via pollen flow in the environment.

In both cases, particles (spores or pollen) must first escape from a plant canopy and enter the planetary boundary layer in order for transport to occur. Long-distance transport will most likely occur during convective conditions, under which a fraction of the particles are rapidly transported to the top of the convective boundary layer (CBL) in updrafts and then eventually mixed throughout the depth of the layer.

The details of particle movement in and above the crop canopy can be adequately described by existing surface layer (SL) Lagrangian stochastic (LS) models. We have developed such a model (Aylor and Flesch 2001; Aylor et al. 2003) and have tested it against maize pollen measurements (Aylor et al. 2006). Our model combines a LS model of particle trajectories in the crop canopy and adjacent atmospheric surface layer with a detailed representation of the canopy that allows deposition on the various parts of the plant and ground to be modeled in detail.

We have also developed a LS model appropriate for transport in the CBL (Boehm and Aylor 2005) based largely on the model described by Luhar (2002). This model has been constructed to mimic the skewed, inhomogeneous turbulence and long time-scales that are characteristic of the CBL.

* *Corresponding author address:* Matthew T. Boehm, Dept. of Plant Pathology and Ecology, The Connecticut Agricultural Experiment Station, P. O. Box 1106, New Haven, CT 06504-1106; e-mail Matthew.Boehm@po.state.ct.us.

We will describe a method for using these two models in combination to study the transport of particles released near the surface for downwind distances of up to several kilometers under conditions ranging from nearly calm and highly convective to windy and neutral or stable. A direct approach to matching the two models by equating turbulence statistics at some matching height is not straightforward because of the fundamental differences in physical processes governing vertical transport in the two cases.

2. MODEL PARAMETERS

In the SL LS model, vertical transport is driven largely by mechanical turbulence generated by friction at the surface. The most important atmospheric parameters in this model are the surface momentum flux and the surface heat flux. These parameters are combined to produce the friction velocity, u_*, and Monin-Obukhov length, L, as the primary inputs into the model. The SL model is generally valid near the ground where $|z/L| << 1$. Thus, the SL model by itself should only be used to study transport up to heights on the order of $|L|$.

In the CBL LS model, vertical transport is due to buoyancy driven turbulence generated in response to surface heating. The relevant atmospheric parameters in this model are the surface heat flux and boundary layer depth, z_i. These two parameters are combined to produce the convective velocity scale, w^*, which joins z_i as an input parameter for the model. The CBL model is valid through the depth of the boundary layer under convective conditions. However, except under the most extreme convective conditions when $-L$ is only a few meters, the SL model is the model of choice near the surface because of its ability to describe the complexities of deposition and air flow in the canopy.

Our intended application of the models is to the near-surface release of particles with appreciable fall velocity relative to the background flow. In this application, an accurate representation of the fraction of the released particles that become airborne is crucial. This fraction, in turn, depends closely on atmospheric conditions near the

surface, in particular the statistics of the wind velocity.

A key assumption of both models is that the atmospheric conditions are steady during the averaging periods over which the model input turbulence parameters are calculated. In addition, the SL model assumes Gaussian probability distribution functions (PDFs) for the three components of the wind velocity: *u*, the component along the mean wind direction for the period; *v*, the component perpendicular to this direction; and *w*, the vertical component. In contrast, the CBL model allows for the skewed, leptokurtic (kurtosis > 3) turbulence that is a key characteristic of the vertical wind component under convective conditions (Luhar et al. 1996 and references therein).

3. DATA ANALYSIS

To examine the validity of these two assumptions under field conditions, we analyzed high-frequency (~21 Hz) data from a sonic anemometer located about 3.2 m above the surface collected on 4 days in 2004 and 7 days in 2005 near Harford, NY. On these days, data were collected for a continuous period of between 3 and 6 hours from mid-morning through mid-afternoon. To study the impact of the averaging period, we analyzed the data over both 2- and 30-minute periods. The wind vector for each data point for a given period was first rotated into the direction of the mean wind for the period. Then, based on these rotated values of *u*, *v*, and *w*, the mean (*U*; the other two components have mean zero after rotation), standard deviation (σ_u, σ_v, and σ_w), skewness (S_u, S_v, and S_w), and kurtosis (K_u, K_v, and K_w) of each wind component over the period were calculated.

Table 1 summarizes the data collected. The "2min" and "30min" daily values for u^* and *L* were calculated from the temperature, momentum flux, and heat flux averaged over all the 2- and 30-minute periods, respectively, on the given day. The last four columns give the mean and standard deviations of *u*, also averaged over all 2- and 30-minute periods. Based on the average values for u^*, and *L*, experiments 3, 4, 5, 6, and 11 can be classified as highly convective with light winds; 2, 8, and 10 as moderately convective with moderate winds; and 1, 7, and 9 as slightly convective days with relatively strong winds.

The length of the averaging time has a relatively minor impact on *U*, u^*, and *L*. Increasing the averaging time always leads to a decrease in *U* because each 2-minute sub-interval is rotated into the direction that maximizes its value for *U*, so that the average over all these sub-intervals must be greater than the value obtained by rotating the 30-minute value. The impact on u^*, and *L* is not quite so well defined, and increasing the averaging time leads to increases in some cases and decreases in others. The biggest impact on these quantities occurs under light wind conditions, when the wind direction is most variable.

The biggest impact of the averaging time can be seen in the values for σ_u. The daily average values for σ_u are significantly greater for 30-minute than for 2-minute averaging times. With each day weighted equally, the average σ_u over 2-minute periods is 0.67, while the corresponding average over 30-minute periods is 0.94. This increase in σ_u with increasing averaging time is due to changes in the mean wind speed from one 2-minute averaging period to the next.

In the SL model, σ_u is parameterized based on u^* and *L*. We found that the parameterized values for σ_u agree more closely with the calculations over the 2-minute periods than over the 30-minute periods. Thus, the SL model appears to be well-tuned to calculate horizontal dispersion over short time-scales.

Table 2 gives the daily average statistics of the vertical velocity PDF, calculated in a similar manner to the horizontal velocity statistics given in Table 1. Table 2 shows that the dependence on averaging period is much less for σ_w than it was for σ_u. This lack of dependence is due to the lack of change in the mean *w* from period to period since W=0 for each period after rotation. With each day weighted equally, the average σ_w over 2-minute periods is 0.34, while the corresponding average over 30-minute periods is 0.35. We found very good agreement between the measurements of σ_w and the parameterization used in the SL model.

The analysis thus far shows that the standard deviations of the horizontal and vertical wind components are parameterized well in the SL model based on u^* and *L* values averaged over 30-minute periods. These values for σ_u and σ_w define the Gaussian velocity PDFs at the foundation of the LS model.

However, under convective conditions the vertical velocity PDF is in general not Gaussian (Luhar et al. 1996). Rather, it is positively skewed with kurtosis greater than 3 (leptokurtic). These

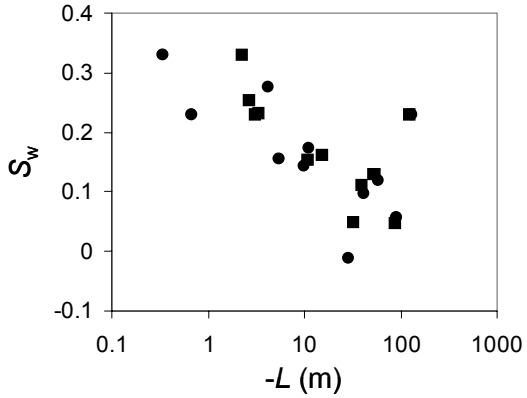

Figure 1. Daily average vertical velocity skewness plotted as a function of Monin-Obukhov length. Calculated based on the 21-Hz sonic anemometer data summarized in Tables 1 and 2. The squares and circles represent values calculated over 2- and 30-minute averaging periods, respectively.

PDF properties are characteristic of intermittency, with periods of light wind punctuated by short periods of stronger wind. Therefore, we calculated the skewness and kurtosis of the wind PDFs to test the assumption of Gaussian turbulence employed by the SL model.

We focus on vertical velocity in these calculations, since w is most important in determining the fraction of particles that escape from the canopy under given weather conditions. Table 2 shows that the skewness, S_w, is typically positive and that in general the length of the averaging period has little impact. Figure 1 shows that S_w increases with increasing instability (decreasing $|L|$). This positive vertical velocity skewness under convective conditions is consistent with measurements and the parameterization used in the CBL model (Luhar et al. 1996).

Table 2 shows that the daily average K_w is leptokurtic for all the days considered here. In addition, K_w is significantly greater over 30-minute than over 2-minute averaging periods. This dependence on averaging period is related to variability in σ_w from one 2-minute averaging period to the next. To show this, we calculated for several of the 30-minute averaging periods the normal distributions corresponding to the σ_w values for each of the 15 2-minute periods that comprise the 30-minute period. These 15 distributions were then averaged to produce a distribution based on the 2-minute data that is representative of the 30-minute period. The resulting average distributions typically had a standard deviation similar to that obtained when averaging was done over the 30-minute and a kurtosis much greater than 3, the kurtosis for each of the individual normal distributions.

The positively skewed and leptokurtic distribution of vertical velocity near the surface under convective conditions yields greater numbers of air parcels moving upwards at high speeds in the positive tail of the distribution than would be predicted by the SL model using the appropriate value for σ_w. This underprediction of air parcels in the positive tail by the SL model would then lead to an underprediction of the number of particles that would become airborne under convective conditions.

The skewness and kurtosis of u were also calculated (not shown). It was found that S_u is sometimes slightly positive, especially under less unstable conditions (i.e. large $|L|$), with average values of 0.12 and 0.18 for the 2- and 30-minute averaging periods, respectively; while K_u is generally less than 3 (platykurtic condition) with average values over all the experiments of 2.74 and 2.90 for the 2- and 30-minute averaging periods, respectively. This slight deviation from Gaussianity in the horizontal velocity is expected to have a smaller impact on results than the dependence of σ_u on the length of the averaging period.

4. MODEL COUPLING

We now discuss the implications of this data analysis to coupling the SL and CBL LS models. Except under highly convective conditions, the SL model will be used to describe the initial motion of particles upon release within the crop canopy. The fraction of particles that become airborne will then be used to help formulate the lower boundary conditions for the CBL model run that will describe the transport over greater distances.

Under light wind conditions in the LS model, a large fraction of the particles have a tendency to fall out and be deposited almost immediately upon release. This is especially true for heavy particles when v_S/σ_w is ~ O(1). Under such light wind conditions, the wind flow tends to be intermittent, with periods of relative calm punctuated by short bursts of more energetic wind. Many biological particles depend on these intermittent wind gusts to be liberated from the plant canopy (Aylor 1990; Shaw et al. 1979). As a result, it is necessary to examine the frequency and intensity of such wind gusts and also to consider how to incorporate them in a consistent manner into the SL model.

In our data analysis, we calculated PDFs of the vertical velocity over 30-minute periods and found that under convective, light-wind conditions the PDF tends to be positively skewed and leptokurtic. Both of these factors lead to an enhancement in the vertical velocity probability density in the positive tail of the distribution relative to the probability density at these velocities in the normal distribution with the same σ_w. We believe that these relatively rare upward moving trajectories are responsible for a significant portion of the airborne fraction that we observed during our field experiment under light-wind conditions, and therefore the effects of positive skewness and leptokurtic kurtosis need to be incorporated into the SL model to accurately model the initial trajectories of particles under convective conditions. However, it is not clear how this will be accomplished, as the SL model equations were derived for Gaussian turbulence and the extension to more general turbulence in the 2D case is not trivial. As mentioned previously, part of the solution likely lies in breaking the data into smaller subintervals so that the period average *w* PDF has greater kurtosis than the PDF obtained based only on the value of σ_w for the entire period. However, this still does not introduce the positive skewness that we measured, and this is an area of continuing work.

The importance of the positive tail is significantly reduced when considering weightless tracer particles compared to heavy particles, since weightless particles simply require a positive vertical velocity to move upward. In addition, weightless particles are typically reflected at the surface, so that the problem of losing most particles to deposition is not an issue.

We are in the process of performing a series of model runs to compare the behavior of the two models under a variety of atmospheric and model boundary conditions. These tests will be used to help formulate a detailed plan for coupling the two models, with an emphasis on the initial behavior of the particles released.

One model parameter that will be examined in particular detail is the Lagrangian time-scale. This time-scale is much larger in the CBL model than in the SL model. As a result, particles that have sufficient release velocity to overcome particle settling have a better chance of maintaining this motion long enough to reach high heights in the CBL model than in the SL model. Perhaps increasing the time-scale in the SL model under highly convective conditions will be necessary to more accurately describe the escape fraction.

The final step will be to compare results obtained using the resulting suite of models with measurements of maize pollen obtained during July 2005 at downwind distances up to several km and heights up to several hundred meters.

5. REFERENCES

Aylor, D. E., 1990: The role of intermittent wind in the dispersal of fungal pathogens. *Ann. Rev. Phytopathology*, **28,** 73-92.

Aylor, D. E., and T. K. Flesch, 2001: Estimating spore release rates using a Lagrangian stochastic model. *J. Appl. Meteorol.,* **40,** 1196-1208.

Aylor, D. E., M. T. Boehm, and E. J. Shields, 2006: Quantifying aerial concentrations of maize pollen in the atmospheric surface layer using remote-piloted airplanes and Lagrangian stochastic modeling. *J. Appl. Meteorol. and Clim.,* in press.

Aylor, D. E., N. P. Schultes, and E. J. Shields, 2003: An aerobiological framework for assessing cross-pollination in maize. *Agricultural and Forest Meteorology,* **119,** 111-129.

Boehm, M. T., and D. E. Aylor, 2005: Lagrangian stochastic modeling of heavy particle transport in the convective boundary layer. *Atmos. Environ.,* **39,** 4841-4850.

Luhar, A. K., 2002: The influence of vertical wind direction shear on dispersion in the convective boundary layer, and its incorporation in coastal fumigation models. *Boundary-Layer Meteorology,* **102,** 1-38.

Luhar, A. K., M. F. Hibberd, and P. J. Hurley, 1996: Comparison of closure schemes used to specify the velocity PDF in Lagrangian stochastic dispersion models for convective conditions. *Atmos. Environ.,* **30,** 1407-1418.

Shaw, R. H., D. P. Ward, and D. E. Aylor, 1979: Frequency of occurrence of fast gusts of wind inside a corn canopy. *J. Appl. Meteorol.,* **18,** 167-171.

Exp	Date	Time (EDT)	u^*_{2min}	u^*_{30min}	L_{2min}	L_{30min}	U_{2min}	U_{30min}	$\sigma_{u,2min}$	$\sigma_{u,30min}$
1	7/30/04	1030-1430	0.47	0.50	-122.6	-132.4	3.9	3.8	1.11	1.26
2	8/01/04	830-1530	0.25	0.26	-39.0	-41.8	2.1	2.0	0.60	0.82
3	8/02/04	830-1600	0.14	0.09	-3.4	-0.7	1.3	1.1	0.48	0.71
4	8/03/04	940-1440	0.16	0.17	-10.8	-9.9	1.4	1.2	0.47	0.77
5	7/21/05	1030-1330	0.08	0.11	-3.1	-5.6	1.0	0.9	0.27	0.53
6	7/22/05	900-1400	0.10	0.11	-2.7	-4.2	1.4	1.2	0.35	0.63
7	7/23/05	900-1500	0.36	0.38	-53.6	-59.0	4.2	4.1	0.96	1.19
8	7/24/05	900-1400	0.22	0.21	-15.4	-11.4	1.9	1.7	0.58	0.88
9	7/25/05	900-1500	0.41	0.42	-87.0	-89.9	5.0	5.0	1.14	1.40
10	7/27/05	930-1300	0.23	0.23	-32.4	-29.2	2.5	2.4	0.81	1.08
11	7/28/05	930-1500	0.14	0.08	-2.3	-0.3	1.8	1.5	0.64	1.04

Table 1. Statistics of 21-Hz data collected during 2004 and 2005 on field experiments near Harford, NY. The subscripts “2min” and “30min” refer, respectively, to the use of 2-minute and 30-minute averaging periods. See text for more details.

Exp	u^*_{2min}	u^*_{30min}	L_{2min}	L_{30min}	$\sigma_{w,2min}$	$\sigma_{w,30min}$	$S_{w,2min}$	$S_{w,30min}$	$K_{w,2min}$	$K_{w,30min}$
1	0.47	0.50	-122.6	-132.4	0.54	0.55	0.23	0.23	3.56	3.75
2	0.25	0.26	-39.0	-41.8	0.35	0.36	0.11	0.10	3.28	3.66
3	0.14	0.09	-3.4	-0.7	0.27	0.28	0.23	0.23	3.26	3.78
4	0.16	0.17	-10.8	-9.9	0.26	0.28	0.15	0.14	3.32	3.84
5	0.08	0.11	-3.1	-5.6	0.17	0.19	0.23	0.16	3.12	3.48
6	0.10	0.11	-2.7	-4.2	0.21	0.22	0.25	0.28	3.55	3.94
7	0.36	0.38	-53.6	-59.0	0.45	0.46	0.13	0.12	3.69	3.93
8	0.22	0.21	-15.4	-11.4	0.30	0.31	0.16	0.17	3.40	3.87
9	0.41	0.42	-87.0	-89.9	0.52	0.54	0.05	0.06	3.72	4.09
10	0.23	0.23	-32.4	-29.2	0.36	0.38	0.05	-0.01	4.07	4.66
11	0.14	0.08	-2.3	-0.3	0.31	0.32	0.33	0.33	3.33	3.71

Table 2. Statistics of 21-Hz data collected during 2004 and 2005 on field experiments near Harford, NY. The subscripts “2min” and “30min” refer, respectively, to the use of 2-minute and 30-minute averaging periods. See text for more details.